Rotational excitation of 20 levels of para–H2O by ortho–H2 (j2=1, 3, 5, 7) at high temperature

F. Daniel, M.L. Dubernet, F. Pacaud, Alain Grosjean

A&A 517, A13 (2010)
DOI: 10.1051/0004-6361/200913745

Astronomy & Astrophysics

Rotational excitation of 20 levels of para-H_2O by ortho-H_2 (j_2 = 1, 3, 5, 7) at high temperature

F. Daniel[1], M.-L. Dubernet[2,3], F. Pacaud[2], and A. Grosjean[4]

[1] Departamento Molecular and Infrared Astrophysics, Consejo Superior de Investigaciones Cientificas, C/ Serrano 121, 28006 Madrid, Spain
[2] Université Pierre et Marie Curie, LPMAA UMR CNRS 7092, Case 76, 4 Place Jussieu, 75252 Paris Cedex 05, France
e-mail: marie-lise.dubernet-tuckey@upmc.fr
[3] Observatoire de Paris, LUTH UMR CNRS 8102, 5 Place Janssen, 92195 Meudon, France
[4] Institut UTINAM, UMR CNRS 6213, 41 bis avenue de l'Observatoire, BP 1615, 25010 Besançon Cedex, France

Received 26 November 2009 / Accepted 16 February 2010

ABSTRACT

Aims. The objective is to obtain the best possible set of rotational (de)-excitation state-to-state and effective rate coefficients for temperatures up to 1500 K. State-to-state rate coefficients are presented among the 20 lowest levels of para-H_2O with $H_2(j_2 = 1)$ and $\Delta j_2 = 0, +2$, and among the 10 lowest levels of para-H_2O with $H_2(j_2 = 3)$ and $\Delta j_2 = 0, -2$.
Methods. Calculations are performed with the close coupling (CC) method over the whole energy range, using the same 5D potential energy surface (PES) as the one employed in our latest publications on water. We compare our CC results both with thermalized quasi-classical trajectory (QCT) calculations using the same PES and with previous quantum calculations obtained between $T = 20$ K and $T = 140$ K with a different PES.
Results. Comparisons with thermalized QCT calculations show factors from 1 to 3. Until recently the only other available set of rate coefficients were scaled collisional rate coefficients obtained with He as a collision partner, and differences between CC and scaled results are shown to be greater than with QCT calculations. The use of the CC accurate sets of rate coefficients might lead to re-estimation of water abundance in the astrophysical whenever models include the scaled H_2O–He rate coefficients.

Key words. molecular data – molecular processes – ISM : molecules

1. Introduction

This is the second publication from the large-scale effort carried out to obtain the highest possible accuracy for collisional excitation rate coefficients of H_20 with rotationally excited H_2. Our previous paper (Dubernet et al. 2009) provided state-to-state rate coefficients among the 45 lowest levels of ortho-H_2O with para-H_2 ($j_2 = 0$) and $\Delta j_2 = 0, +2$, as well as with $j_2 = 2$ and $\Delta j_2 = 0, -2$. In addition to and only for the 10 lowest energy levels of ortho-H_2O did Dubernet et al. (2009) obtain state-to-state rate coefficients involving $j_2 = 4$ with $\Delta j_2 = 0, -2$ and $j_2 = 2$ with $\Delta j_2 = +2$.

Those efforts for the excitation of water are justified by the importance of water in various astrophysical media. Water is a key molecule for the chemistry and the energy balance of the gas in cold clouds and star-forming regions, thanks to its relatively large abundance and large dipole moment.

The Heterodyne Instrument for the Far-Infrared (HIFI) was launched in May 2009 on board the Herschel Space Observatory, publication of the water rate coefficients becomes urgent. The instrument will observe spectra of many molecules with unprecedented sensitivity with an emphasis on water lines in regions such as low- or high-mass star-forming regions, proto-planetary disks, and AGB stars. The interpretation of these spectra will rely upon the accuracy of the available collisional excitation rate coefficients that enter into the population balance of the emitting levels of the molecules. In the temperature range from 5 K to 1500 K, the most abundant collider likely to excite molecules in media with weak UV radiation fields is the hydrogen molecule, followed by the helium atom.

The present paper investigates the excitation of the 20 lowest para-H_20 rotational levels by ortho-H_2 ($j_2 = 1, 3, 5, 7$) for kinetic temperatures from 5 K to 1500 K. It extends the work of Dubernet et al. (2006), which provided rate coefficients for de-excitation of the lowest 10 rotational levels of ortho/para-H_2O by collisions with para-H_2 ($j_2 = 0$) and ortho-$H_2(j_2 = 1)$. Present and past Dubernet et al. (2006, 2009) quantum dynamical calculations were carried out with the 5D potential energy surface (PES) determined by Faure et al. (2005). This accurate 5D PES, suitable for inelastic rotational calculations, was obtained from a 9D PES by averaging over H_2 and H_2O ground vibrational states. As pointed out in Faure et al. (2005), this state-averaged PES is actually very close to a rigid-body PES using state-averaged geometries for H_2O and H_2.

Dubernet et al. (2006) showed that the new PES of Faure et al. (2005) have led to a significant re-evaluation of the rate coefficients for the excitation of H_2O by para-H_2 ($j = 0$) below 20 K and to a weak effect with a maximum change of 40% for collisions with ortho-$H_2(j = 1)$ when their results were compared to the collisional calculations of Phillips et al. (1996); Dubernet & Grosjean (2002); Grosjean et al. (2003) obtained with the 5D PES of Phillips et al. (1994).

For the de-excitation of ortho-H_2O by para-H_2 ($j = 0$), Dubernet et al. (2009) compared the effective rate coefficients of Phillips et al. (1996) for the first 10 levels of ortho-H_2O with temperatures in the range 20 K to 140 K. It was shown that the

ratios of effective rate coefficients converge slowly towards unity with temperature, certainly reflecting the decreasing influence of the difference between the two different PES (Phillips et al. 1994; Faure et al. 2005) as temperature increases.

In addition, Dubernet et al. (2009) carried out comparisons with thermalized QCT calculations of Faure et al. (2007) that showed large factors at intermediate temperature and factors from 1 to 3 at high temperature for the strongest rate coefficients. We showed also that scaled collisional rate coefficients obtained with He could not be used in place of collisional rate coefficients with para-H_2. The quantum calculations of Dubernet et al. (2009) pointed out the importance of internal energy transfer between excitation of H_2 and de-excitation of ortho-H_2O, which was at the origin of some large differences observed with QCT calculations of Faure et al. (2007) and with scaled collisional rate coefficients obtained with He (Green et al. 1993).

We recall that Faure et al. (2007) provides rate coefficients for rotational de-excitation among the lowest 45 rotational levels of ortho/para-H_2O colliding with thermalized ortho/para-H_2 in the temperature range 20–2000 K. This set is a combination of various data: 1) data obtained with quasi classical trajectory (QCT) calculations with the H_2 molecule assumed to be rotationally thermalized at kinetic temperature and calculated between 100 K and 2000 K, 2) the values at 20 K are CC calculations from Dubernet et al. (2006) for the first 5 levels and equal to values at 100 K for all other levels, 3) scaled H_2O-He results from Green et al. (1993) for the weakest rate coefficients.

It should be mentioned that calculations of collisional excitation by ortho-H_2 have been carried out solely on 4 diatomic molecules CO (Flower & Launay 1985; Mengel et al. 2001; Flower 2001; Wernli et al. 2006), H_2 (Flower & Roueff 1999b), HD (Flower 1999; Flower & Roueff 1999a), SiS (Kłos & Lique 2008), and on water (Phillips et al. 1996; Grosjean et al. 2003; Dubernet et al. 2006; Faure et al. 2007), and that all quantum calculations except those of Dubernet et al. (2006) restricted the H_2 basis set to $j_2 = 1$.

Our current objective is to obtain the best possible set of rotational (de)-excitation state-to-state and effective rate coefficients for temperatures up to 1500 K. In particular, our basis set for H_2 is extended to $j_2 = 3$, which allows for internal energy transfer between excitation of ortho-H_2 and de-excitation of para-H_2O. We provide state-to-state rate coefficients among the 20 lowest levels of para-H_2O with $H_2(j_2 = 1)$ and $\Delta j_2 = 0, +2$, and among the 10 lowest levels of para-H_2O with $H_2(j_2 = 3)$ and $\Delta j_2 = 0, -2$. We predict the effective rate coefficients for $j_2 = 5,7$.

2. Methodology

2.1. Collisions with H_2

Our calculations provide state-to-state collisional rate coefficients involving changes in both the target and the perturber rotational levels, i.e. $R(j_1\tau_1 j_2 \rightarrow j'_1\tau'_1 j'_2)(T)$ where $j_1\tau_1$ and $j'_1\tau'_1$ represent the initial and final rotational levels of water, j_2 and j'_2 the initial and final rotational levels of H_2, and T is the kinetic temperature.

The state-to-state collisional rate coefficients are the Boltzmann thermal averages of the state-to-state inelastic cross sections:

$$R(j_1\tau_1 j_2 \rightarrow j'_1\tau'_1 j'_2)(T) = \left(\frac{8}{\pi\mu}\right)^{1/2} \frac{1}{(k_B T)^{3/2}} \int_0^\infty \sigma_{j_1\tau_1 j_2 \rightarrow j'_1\tau'_1 j'_2}(E)\, E\, e^{-E/k_B T} dE, \quad (1)$$

where E is the kinetic energy, k_B the Boltzmann constant and μ the reduced mass of the colliding system.

These state-to-state collisional rate coefficients follow the principle of detailed balance, and reverse rate coefficients $R(j'_1\tau'_1 j'_2 \rightarrow j_1\tau_1 j_2)(T)$ can be obtained from forward rate coefficients by the usual formula:

$$g_{j'_1}\, g_{j'_2}\, e^{-\frac{E'_{int}(H_2O)}{k_B T}} e^{-\frac{E'_{int}(H_2)}{k_B T}} R(j'_1\tau'_1 j'_2 \rightarrow j_1\tau_1 j_2) = g_{j_1}\, g_{j_2}\, e^{-\frac{E_{int}(H_2O)}{k_B T}} e^{-\frac{E_{int}(H_2)}{k_B T}} R(j_1\tau_1 j_2 \rightarrow j'_1\tau'_1 j'_2), \quad (2)$$

where g_{j_1} and g_{j_2} are the statistical weights related to rotational levels of H_2O and H_2 respectively, and the different E_{int} are the rotational energies of the species.

Some astrophysical applications might use the so-called effective rate coefficients $\hat{R}_{j_2}(j_1\tau_1 \rightarrow j'_1\tau'_1)$, which are given by the sum of the state-to-state rate coefficients (Eq. (1)) over the final j'_2 states of H_2 for a given initial j_2:

$$\hat{R}_{j_2}(j_1\tau_1 \rightarrow j'_1\tau'_1)(T) = \sum_{j'_2} R(j_1\tau_1 j_2 \rightarrow j'_1\tau'_1 j'_2)(T). \quad (3)$$

These effective rate coefficients do not follow the detailed balance principle, and both excitation and de-excitation should be explicitly calculated.

Finally, averaged de-excitation rate coefficients for para-H_2O by rotationally thermalized ortho-H_2 can be obtained by averaging over the initial rotational levels of ortho-H_2:

$$\overline{R}(j_1\tau_1 \rightarrow j'_1\tau'_1) = \sum_{j_2} \rho(j_2) \hat{R}_{j_2}(j_1\tau_1 \rightarrow j'_1\tau'_1)(T) \quad (4)$$

with $\rho(j_2) = g_{j_2} e^{-\frac{E_{int}(H_2)}{k_B T}}/Z$, where Z is the partition function over either ortho-H_2 states. These averaged de-excitation rate coefficients are those directly calculated by Faure et al. (2007) with a QCT method.

2.2. Description of the calculations

In the current calculations we used the same expansion of the Faure et al. (2005) 5D PES as in Dubernet et al. (2006), where details can be found. For this PES, inaccuracies in inelastic cross sections might come from different sources: propagation parameters, description of the rotational Hamiltonians of the 2 molecules, sizes of H_2O and H_2 rotational basis sets, and a level of approximation in quantum calculations where the coupled states (CS) approximation might be used instead of the exact close coupling (CC) method. Additional errors might be introduced in rate coefficients if the kinetic energy grid is not fine enough near thresholds, resulting in poor low-temperature rate coefficients, or not extended to high enough energies, leading to wrong high-temperature results.

Our quantum calculations were carried out with modified versions of the sequential and parallel versions of the MOLSCAT code (Hutson & Green 1994; McBane 2004). Parameters of the propagation were optimized as in Dubernet & Grosjean (2002); Grosjean et al. (2003); Dubernet et al. (2006), and (Dubernet et al. 2009). Identical to Dubernet et al. (2006, 2009), the H_2 energy levels are the experimental energies of Dabrowski (1984), and the H_2O energy levels and eigenfunctions were obtained by diagonalisation of the effective Hamiltonian of Kyrö (1981), compatible with the symmetries of the PES (Dubernet & Grosjean 2002; Grosjean et al. 2003; Dubernet et al. 2006), and (Dubernet et al. 2009). The first 20 levels of para-H_2O are given in Table 1. The reduced mass of the system is 1.81277373 a.m.u.

Table 1. Energy levels of para-H_2O.[a]

Level	Energy (cm^{-1})	j	τ	k_a	k_c
1	0.0000	0	0	0	0
2	37.1371	1	0	1	1
3	70.0907	2	–2	0	2
4	95.1757	2	0	1	1
5	136.1641	2	2	2	0
6	142.2783	3	–2	1	3
7	206.3013	3	0	2	2
8	222.0529	4	–4	0	4
9	275.4971	4	–2	1	3
10	285.2200	3	2	3	1
11	315.7792	4	0	2	2
12	326.6256	5	–4	1	5
13	383.8427	4	2	3	1
14	416.2088	5	–2	2	4
15	446.6972	6	–6	0	6
16	488.1349	4	4	4	0
17	503.9682	5	0	3	3
18	542.9070	6	–4	1	5
19	586.4800	7	–6	1	7
20	602.7742	6	–2	2	4

Notes. [(a)] obtained with the Kyrö (1981) Hamiltonian.

Table 2. Contribution of the state-to-state rate coefficients $R(j_1\tau_1 j_2 \rightarrow j'_1\tau'_1 j'_2)(T)$ with $j_2 = 1$ to $j'_2 = 3$ to the effective rate coefficients $\hat{R}_{j_2=1}(j_1\tau_1 \rightarrow j'_1\tau'_1)(T)$ for the four largest transitions with $\Delta j_2 = +2$.

Transitions / T(K)	200	400	1000	1500
6_{24} to 4_{22}	9%	24%	38%	42%
6_{15} to 4_{13}	5%	16%	31%	36%
7_{17} to 5_{15}	4%	12%	27%	33%
4_{40} to 2_{20}	7%	16%	24%	27%

2.2.1. Basis set convergence

The methodology in choosing an appropriate basis set is the same of the one described in Dubernet et al. (2009) which should be consulted for additionnal information. The basis set is a direct product of rotational wavefunctions of water, characterized by the rotational quantum number j_1 (the lowest value of j_1 is one for para-H_2O) and the pseudo-quantum number τ_1 which varies between $-j_1$ and j_1 (alternatively, we may use the pseudo-quantum numbers k_a and k_c with the correspondence $\tau_1 = k_a - k_c$), and of rotational wavefunctions of hydrogen characterized by the rotational quantum number j_2. We call $B(n, m)$ a basis set where n is the maximum value of j_1, m is the maximum value of j_2, and $B(n, m)$ includes all the coupled $|j_{12}, j_1, \tau_1, j_2>$ states, with $\hat{j}_{12} = \hat{j}_1 + \hat{j}_2$. The convergence of the basis set usually involves keeping a number of closed channels above the total energy at which the collisional cross-sections are calculated. The potential couplings between $(j_1 k_a k_c)$ energy levels decrease with increasing Δj_1 and Δk_a and we find that a good convergence is reached with 10 energetically closed channels of water.

Another important question is the accuracy of cross-sections with respect to the number of closed channels of the H_2 molecule. Generally at least one to two closed H_2 rotational channels would be required to ensure convergence to better than 5% of inelactic cross sections involving energy transfer in H_2. This would be particularly important if the purpose of our calculations was to find inelastic rate coefficients of H_2 averaged over water transitions. For our calculations, it is sufficient to use a basis set with a maximum value of $j_2 = 3$, expecially as

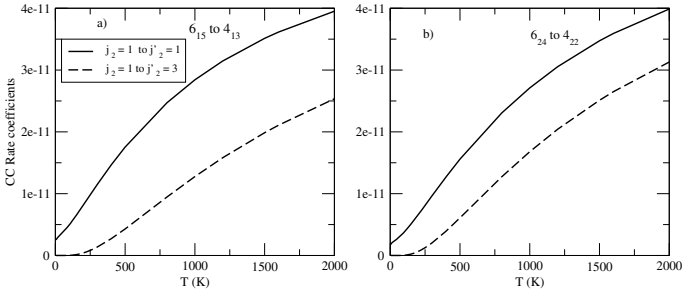

Fig. 1. State-to-state rate coefficients ($cm^3 s^{-1}$) of the 6_{24} to 4_{22} and the 6_{15} to 4_{13} transition of para-H_2O as a function of temperature (Kelvin).The full line indicates the state-to-state rate coefficients for $\Delta j_2 = 0$, and the broken line corresponds to $\Delta j_2 = +2$.

the $j_2 = 5$ level lies 1034.67 cm^{-1} above the $j_2 = 3$ level of ortho-H_2. The inclusion of $j_2 = 3$ leads to small differences for state-to-state rate coefficients of para-H_2O with $H_2(j_2 = 1)$ and $\Delta j_2 = 0$, but it allows the possibility of internal energy transfer between excitation of ortho-H_2 and de-excitation of para-H_2O. Indeed Fig. 1 and Table 2 show examples of transitions of para-H_2O for which the state-to-state rate coefficients with $H_2(j_2 = 1)$ and $\Delta j_2 = +2$ is non negligible compared to the state-to-state rate coefficients with $H_2(j_2 = 1)$ and $\Delta j_2 = 0$.

Finally our choice is a $B(n, m)$ basis set with 10 energetically closed channels of water and an energy cut-off of 1309 cm^{-1} for $|j_{12}, j_1, \tau_1, j_2>$ states connected to $j_2 = 3$.

This ensures very good convergence for the significant state-to-state rate coefficients, i.e., among the 20 lowest levels of para-H_2O with $H_2(j_2 = 1)$ and $\Delta j_2 = 0$, among the 10 lowest levels of para-H_2O with $H_2(j_2 = 3)$ and $\Delta j_2 = 0, -2$, among the 10 lowest levels of para-H_2O with $H_2(j_2 = 1)$ and $\Delta j_2 = +2$, from the 11th-20th levels to the first 13th levels of para-H_2O with $H_2(j_2 = 1)$ and $\Delta j_2 = +2$. A worse convergence is reached for state-to-state rate coefficients among levels between the 14th of 20th levels of para-H_2O with $H_2(j_2 = 1)$ and $\Delta j_2 = +2$. Fortunally, most of the last state-to-state rate coefficients are negligible or very small compared to state-to-state rate coefficients among levels between the 14th of 20th levels of para-H_2O with $H_2(j_2 = 1)$ and $\Delta j_2 = 0$, so the corresponding effective rate coefficients with $H_2(j_2 = 1)$ have good accuracy. Uncertainties linked to convergence of the basis set are part of the total uncertainties indicated in Table 3.

2.2.2. Choice of total energy points

The CC calculations were carried out over essentially the whole energy range spanned by the Boltzmann distributions (Eq. (1)). The highest energy point calculated is at 8000 cm^{-1} and cross sections are extrapolated at higher energy in order to achieve convergence for de-excitation from the highest water energy levels. These extrapolations do not degrade the accuracy of rate coefficients because the concerned cross sections behave regularly. We carefully spanned the energy range above the inelastic channels and added more points in the presence of resonance structures. The energy steps were fixed to 0.1 cm^{-1} for the total energy below 205 cm^{-1}. Between 205 cm^{-1} and 720 cm^{-1} energy steps vary from 0.5 to 1 cm^{-1}, from 720 to 815 cm^{-1} they range from 2 to 5 cm^{-1}, from 815 to 920 cm^{-1} they range from 13 to 30 cm^{-1}, and above 920 they vary up to 500 cm^{-1}. We paid particular attention to having a fine description of low-energy behaviors of cross sections connected to $j_2 = 3$ for the first 10 rotational levels of para-H_2O. Some of the additionnal

Table 3. Summary of the sets of state-to-state rate coefficients (STSR) $R(j_1\tau_1 j_2 \rightarrow j'_1\tau'_1 j'_2)(T)$ available in BASECOL (sets (1), (2), (3), (4) below 10th level), and effective rate coefficients (ER) $\hat{R}_{j_2}(j_1\tau_1 \rightarrow j'_1\tau'_1)(T)$.

Set				$T_{\rm min}$(K)	$T_{\rm max}$(K)	Transitions	$T1$	$T2$
(1)	$j_2 = 1$	$j'_2 = 1$	STSR	5	1500	20 levels	5%	10%
(2a)		$j'_2 = 3$	STSR	300	1500	20 levels	20%	20%–40% (Note)
(2b)		$j'_2 = 3$	STSR	5	300	20 levels	A2	A2
		$\sum_{j'2}$	ER	5	1500	20 levels	5%	15%–20%
(3)	$j_2 = 3$	$j'_2 = 1$	STSR	5	1500	10 levels	A2	
(4)		$j'_2 = 3$	STSR	5	1500	10 levels	10%	
		$\sum_{j'2}$	ER	5	1500	10 levels	15%	

Notes. Column 1 labels the set of state-to-state rate coefficients. $T_{\rm min}$(K) and $T_{\rm max}$(K) indicate the lowest and highest temperatures at which calculations and fits have been performed for the relevant sets of data. The column "Transition" indicates the number of levels among which rate coefficients are provided. $T1$, $T2$ indicate the worst expected accuracy: $T1$ for transitions among the 10 first levels of para-H_2O, $T2$ for de-excitation from the 11th–20th levels. A2 means "not good but negligible". Note: for set (2a) and $T2$, the accuracy is 20% for de-excitation to the first 13th levels and 40% for de-excitation to the 14th–19th levels.

thresholds cross sections connected to $j_2 = 3$ were calculated with the breathing sphere approximation (Agg & Clary 1991a,b), i.e., we averaged the PES over $j_2 = 3$, similarly to what had been done for $j_2 = 4$ in Dubernet et al. (2009). This procedure is fully justified by the small magnitude of cross sections involving energy transfer with $\Delta j_2 = -2$ from $j_2 = 3$. We checked that the resulting breathing sphere cross-sections agreed with sparser cross sections obtained with the accurate basis set described above. Nevertheless, for $j_2 = 3$ at high energy, the energy grid is coarser than for $j_2 = 1$, though still allowing adequate precision (see Table 3). Overall there are about 1192 energy points.

Table 4. Labels of transitions.

Level	First	Last	Level	First	Last
2	1	1	12	56	66
3	2	3	13	67	78
4	4	6	14	79	91
5	7	10	15	92	105
6	11	15	16	106	120
7	16	21	17	121	136
8	22	28	18	137	153
9	29	36	19	154	171
10	37	45	20	172	190
11	46	55			

3. Discussion

3.1. Results for j_2 = 1, 3, 5, 7

We used the methodology described above to calculate sets of state-to-state rate coefficients (Eq. (1)) in the temperature range from 5 K to 1500 K for de-excitation among the 20 lowest levels of para-H_2O with $H_2(j_2 = 1)$ and $\Delta j_2 = 0, +2$, and among the 10 lowest levels of para-H_2O with $H_2(j_2 = 3)$ and $\Delta j_2 = 0, -2$. The state-to-state rate coefficients involving energy transfers from $j_2 = 3$ to $j_2 = 1$ contribute only 4% or less to the effective rate coefficients; nevertheless, we provide them for the sake of completeness. They should only be used to calculate the effective excitation and de-excitation rate coefficients of para-H_2O corresponding to the $j_2 = 3$ level of ortho-H_2 as their accuracy is very low. In addition we obtain de-excitation rate coefficients from the 11th–20th levels of para-H_2O with $H_2(j_2 = 3)$ and $\Delta j_2 = 0$, but we did not try to obtain accurate values so those rate coefficients will not be published.

From the calculated state-to-state rate coefficients, the effective rate coefficients corresponding to j_2= 1, 3 can be calculated using Eq. (3). The ratios of effective de-excitation rate coefficients (Eq. (3)) $\hat{R}_{j_2=3}$ over effective de-excitation rate coefficients $\hat{R}_{j_2=1}$ for the first 10 levels of para-H_2O are given in Fig. 2. Table 4 provides labels of first and last de-excitation transitions from a given level as given in Table 1. This table is the key for reading the figures giving ratios of rate coefficients as a function of transitions labels. The first transition from level n is the transition $n \rightarrow 1$, the last transition is the transition $n \rightarrow n-1$. Ratios $\hat{R}_{j_2=3}/\hat{R}_{j_2=1}$ are generally close to 1 within a maximum variation of 20%, except at low temperature for the weakest transitions from levels 6, 7, 8 (see Table 1) to the ground state. Because of the weakness of transitions and because those stronger ratios occur at low temperature where $j_2 = 3$ is unlikely to be important in most application cases, the difference between $j_2 = 1$ and $j_2 = 3$ is not significant for astrophysical applications. We can assume that effective rate coefficients $\hat{R}_{j_2=5}$, $\hat{R}_{j_2=7}$ will be close to $\hat{R}_{j_2=1}$.

The BASECOL database (Dubernet et al. 2006) provides full tables of the rate coefficients sets mentioned in Table 3, i.e. sets (1), (2), (3), and (4).

3.2. Accuracy of results

Apart from the usual checks of convergence with respect to propagation parameters, basis set, and total angular momentum, the state-to-state rate coefficients have been carefully checked by detailed balance. It should be recalled that the quality of rate coefficients at low temperature is linked to the number of energy points close to the molecular thresholds, and we have an excellent energy grid for both $j_2 = 1$ (20 levels of para-H_2O) and $j_2 = 3$ (10 levels of para-H_2O). The maximum values of the estimated errors are given in Table 3 for transitions starting from different levels of para-H_2O (T1, T2) and for the various sets of state-to-state rate coefficients (1 to 4). Set (2a) shows very good accuracy for transitions among the first 10 levels of para-H_2O and for transitions from the 11th-20th levels to the first 10 levels of para-H_2O. Set (2b) has lower accuracy, but this is no concern because this set does not contribute significantly to the effective rate coefficients. Set (3) has very low accuracy, which is not a cause for concern for the present application since they provide a very negligible contribution to the effective rate coefficients. The accuracy of the effective rate coefficients (ER) $\hat{R}_{j_2=1}$ reflects the accuracies of set (1) and of sets (2). The accuracy of the effective rate coefficients (ER) $\hat{R}_{j_2=3}$ is mainly connected to

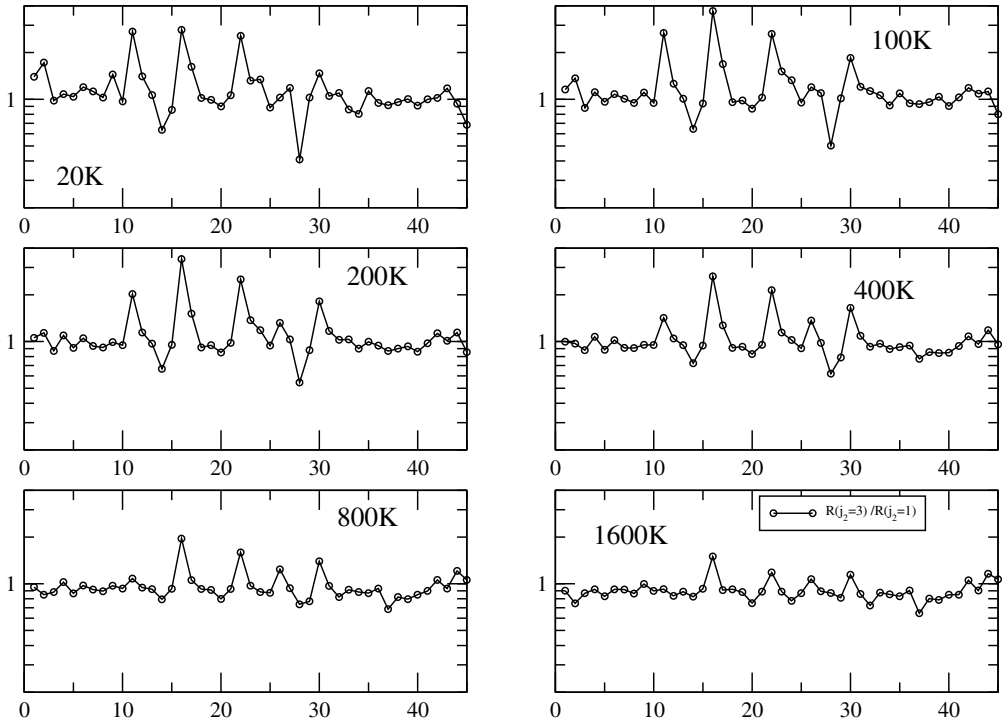

Fig. 2. Ratios of effective de-excitation rate coefficients $\hat{R}_{j_2=3}/\hat{R}_{j_2=1}$ (Eq. (3)) for the first 10 levels of para-H_2O and for temperatures ranging from 20 K to 1600 K. The abscissae indicate the labeling of the de-excitation transitions as indicated in Table 4.

set (4) because set (3) rate coefficients give a small contribution to the effective rate coefficients.

3.3. Thermalized rate coefficients

We do not explicitly provide de-excitation rate coefficients of para-H_2O with thermalized H_2 (Eq. (4)). $j_2 = 3$ makes a significant contribution around 300–400 K and that $j_2 = 5$ starts to contribute significantly around 1000 K. Therefore our calculations can provide highly accurate averaged de-excitation rate coefficients (Eq. (4)) up to 400 K for transitions from the 20 first levels of para-H_2O, up to 1000 K for transitions from the first 10th level of para-H_2O, the accuracy being connected to accuracies listed in Table 3. We showed that $j_2 = 3$ significant effective rate coefficients are very close to $j_2 = 1$, therefore we can safely assume all unknown $j_2 = 3, 5, 7$ significant effective rate coefficients to be close to $j_2 = 1$ in calculating the thermalized rate coefficients. Another possibility at high temperature and high levels of water is to directly use the QCT rate coefficients of Faure et al. (2007), but to be aware of their limitation. Comparisons between our averaged de-excitation rate coefficients and the QCT results are given in the following sections.

3.4. Comparison with QCT and scaled He calculations

To compare the quantum and QCT results obtained with the same PES, we must remove the scaled H_2O-He results of Green et al. (1993) from their published set since they cover a large fraction of the transitions over a range of temperatures. The averaged CC rate coefficients in Fig. 3 include our unpublished state-to-state rate coefficients corresponding to the extension of sets (3) and (4) of Table 3 above the 11th level of para-H_2O. These unpublished state-to-state rate coefficients have a maximum accuracy of 50%. The de-excitation rate coefficients of H_2O + He of Green et al. (1993), scaled by a factor of 1.344 to correct for the differing colliding system masses, have systematically been used in astrophysical applications to mimic rate coefficients of H_2O + H_2. Phillips et al. (1996) pointed out that this method is not valid for temperatures up to 140 K. We note that the CC and QCT rate coefficients are within a factor of 3 over the temperature range with ratios around 1, whereas scaled He calculations mostly underestimate CC rate coefficients. The agreement between CC and He scaled calculations gets better with increasing temperature. These figures do not include He scaled transitions that lead to very high ratios, i.e., transitions starting from some level n to level 1.

Figures 4 to 6 compare our averaged rate coefficients with those of Faure et al. (2007) and with scaled He rate coefficients of (Green et al. 1993) for de-excitation transitions from the first 16 levels of para-H_2O at 200 K. These last two sets coincide for some transitions since the Faure et al. (2007) set includes both QCT calculations and scaled He rate coefficients for the weakest transitions. Overall we find that the QCT calculations give better absolute values than scaled He calculations.

3.5. Comparison with the H_2O + H_2 effective rate coefficients of Phillips et al. (1996)

Comparison with effective rate coefficients of Phillips et al. (1996) can only be performed for the first 10 levels of para-H_2O and for temperatures in the range 20 K to 140 K. It is recalled that between 20 K and 140 K, effective rate coefficients (Eq. (3)) for $j_2 = 1$ are equal to averaged rate coefficients (Eq. (4)) since j_3 is scarcely populated. The ratios of effective rate coefficients given in Table 5 are very close to 1 for the strongest transitions and do not have a strong temperature dependence. Overall the new PES of Faure et al. (2005) does not induce a significant change in rate coefficients for collision with ortho-H_2.

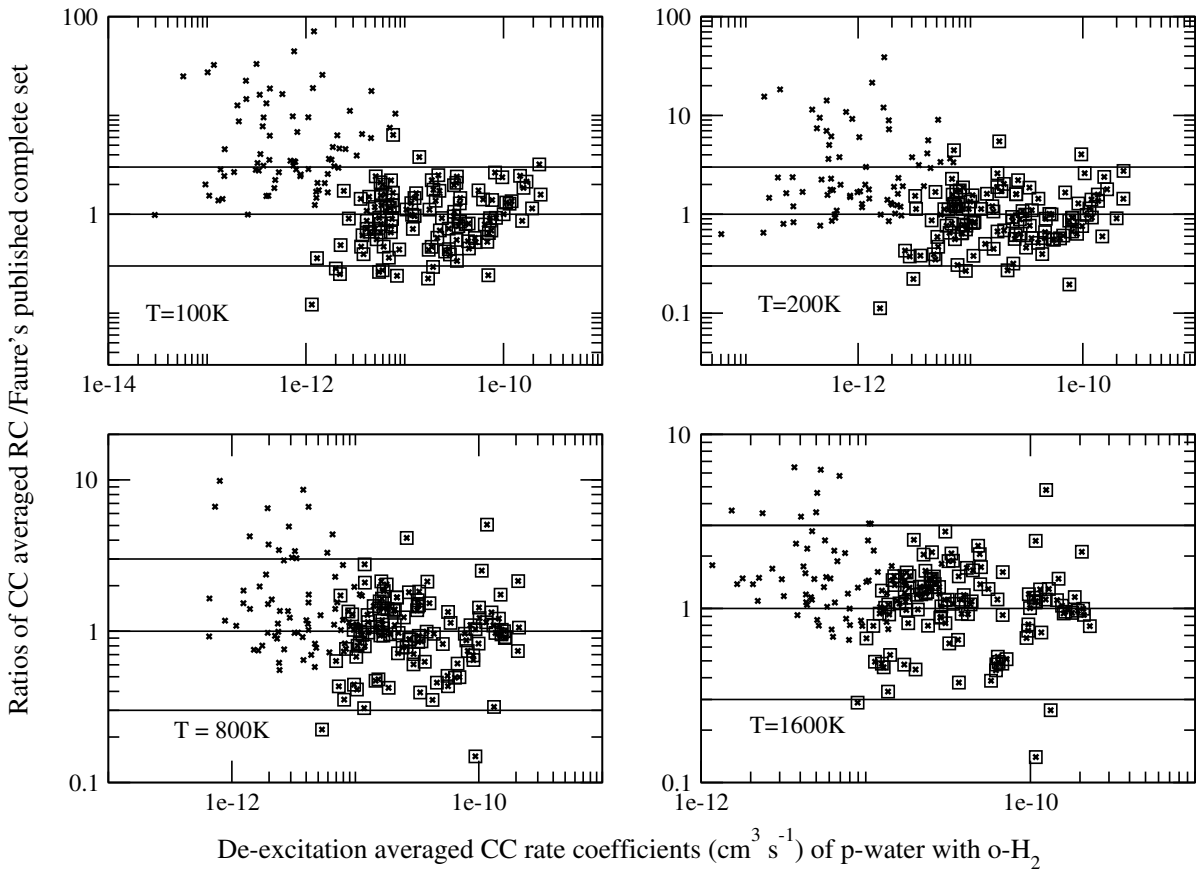

Fig. 3. Ratios of CC averaged de-excitation rate coefficients (Eq. (4)) of para-H_2O with ortho-H_2 over data sets published by Faure et al. (2007) as a function of the CC averaged de-excitation rate coefficients of para-H_2O with ortho-H_2 (in cm^3s^{-1}). These data sets include both the quasi-classical calculations (crosses in squares) and scaled water-He rate coefficients (crosses without squares) published in Faure et al. (2007).

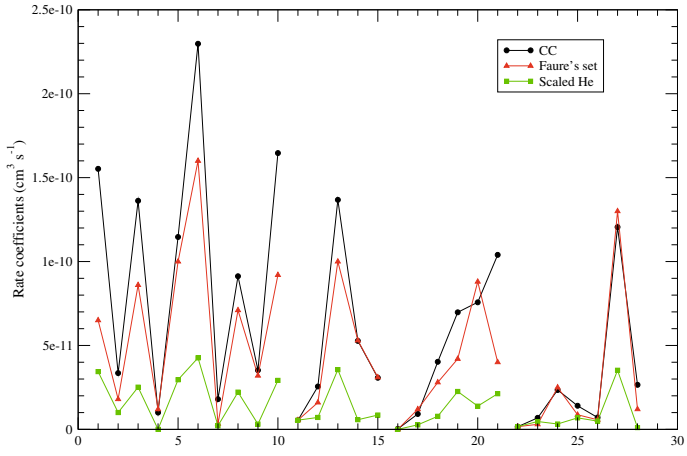

Fig. 4. CC averaged de-excitation rate coefficients (Eq. (4)) of para-H_2O with ortho-H_2, set of rate coefficients published by Faure et al. (2007) (black line) and scaled He rate coefficients of (Green et al. 1993) (red line) at 200 K for the 1st to the 28th de-excitation transitions. The abscissae indicate the labeling of the de-excitation transitions as indicated in Table 4.

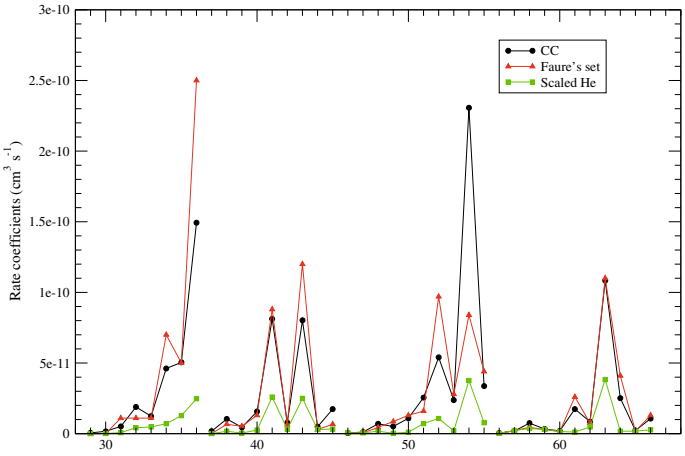

Fig. 5. CC averaged de-excitation rate coefficients (Eq. (4)) of para-H_2O with ortho-H_2, set of rate coefficients published by Faure et al. (2007) (black line) and scaled He rate coefficients of (Green et al. 1993) (red line) at 200 K for the 29th to the 66th de-excitation transitions. The abscissae indicate the labeling of the de-excitation transitions as indicated in Table 4.

3.6. Fitted rate coefficients

The state-to-state rate coefficients $R(j_1\tau_1 j_2 \rightarrow j_1'\tau_1' j_2')(T)$ for the de-excitation of para-H_2O with para-H_2 ($j_2 = 1, 3$) and $\Delta j_2 = 0, \pm 2$ are fitted to an analytical form very similar to the one used by Mandy & Martin (1993):

$$\log_{10} R(T) = \sum_{k=1}^{N-1} a_k \left[\log_{10} \frac{T}{\epsilon}\right]^{k-1} + a_N \left(\frac{1}{T/\epsilon + \epsilon} - 1\right). \quad (5)$$

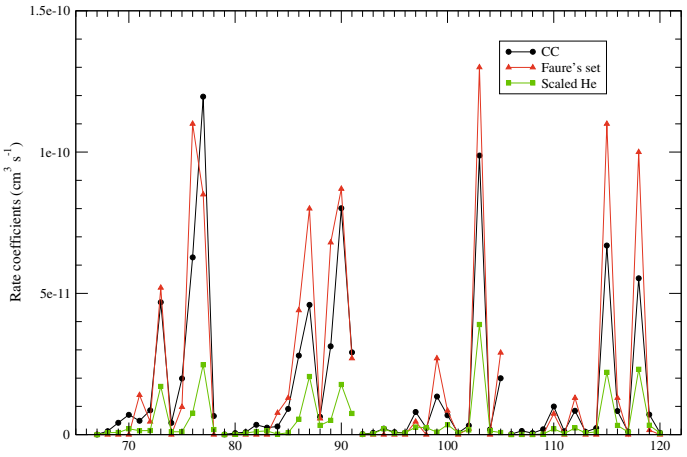

Fig. 6. CC averaged de-excitation rate coefficients (Eq. (4)) of para-H_2O with ortho-H_2, set of rate coefficients published by Faure et al. (2007) (black line) and scaled He rate coefficients of (Green et al. 1993) (red line) at 200 K for the 67th to the 190th de-excitation transitions. The abscissae indicate the labeling of the de-excitation transitions as indicated in Table 4.

Table 5. Ratios of the 5 effective de-excitation rate coefficients of Phillips et al. (1996) over our effective rate coefficients (Eq. (3)) for $j_2 = 1$ (equal to our averaged rate coefficients).

T (K)	20	40	60	80	100	120	140
Transitions							
2 1	1.13	1.08	1.06	1.05	1.04	1.03	1.03
3 1	1.10	1.07	1.06	1.05	1.04	1.04	1.04
3 2	1.11	1.11	1.12	1.12	1.12	1.11	1.11
4 1	1.76	1.65	1.60	1.57	1.53	1.51	1.48
4 2	1.16	1.09	1.06	1.05	1.04	1.02	1.01
4 3	0.99	1.00	1.00	0.99	0.98	0.96	0.94
5 1	1.44	1.40	1.39	1.41	1.43	1.46	1.47
5 2	1.35	1.33	1.33	1.35	1.38	1.42	1.45
5 3	1.32	1.30	1.28	1.25	1.22	1.18	1.16
5 4	1.06	1.06	1.07	1.08	1.08	1.08	1.08

The fits were performed using numerical rate coefficients calculated at ∼100 temperatures ranging from $T_{\rm min}$ to $T_{\rm max}$, which are indicated in Table 3. The fitted coefficients are such that the maximum error between initial data points and fitted values is minimal. A maximum value of $N = 14$ is needed for good accuracy over the whole range of temperature. The fitted rate coefficients were subsequently compared to numerical rate coefficients calculated with a step of $T = 1$ K from $T_{\rm min}$ to $T_{\rm max}$, and the maximum error found is less than 0.5%. We emphasize that these fits have no physical meaning; they are only valid in the temperature range of the relevant $T_{\rm min}$, $T_{\rm max}$ and should not be used to perform extrapolations. The complete fitting coefficients sets corresponding to sets (1), (2a,b), (3), and (4) of Table 3 will be available in the BASECOL database (Dubernet et al. 2006). The quality of the fits can be checked online through the graphic interface.

4. Concluding remarks

We provide state-to-state rate coefficients among the 20 lowest levels of para-H_2O with $H_2(j_2 = 1)$ and $\Delta j_2 = 0, +2$ and among the 10th levels of para-H_2O with ortho-$H_2(j_2 = 3)$ and $\Delta j_2 = 0, -2$. We predict the effective rate coefficients for $j_2 = 5, 7$.

For the given PES, the accuracy of quantum rate coefficients, explicitly given for different temperatures and transitions, is rather homogeneous and lies between 5% and 40% for the first 20 levels of para-H_2O. For the available transitions and temperature, we strongly recommend using the present sets of effective rate coefficients instead of either the scaled H_2O-He data of Green et al. (1993) or the set published in Faure et al. (2007). For the uncalculated effective rate coefficients with $j_2 = 3, 5, 7$, the user might use guesses as explained in Sect. 3.3. Alternatively, the user may use the sets of thermalized rate coefficients published in Faure et al. (2007), being aware that the weakest transitions are given by scaled H_2O-He rate coefficients that are sometimes wrong by large factors. We find that the scaled He rate coefficients (Green et al. 1993) are representative neither of the effective rate coefficients $\hat{R}_{j_2=1}$ nor of the averaged CC rate coefficients in absolute values.

Collisions with ortho-H_2 ($j_2 = 1$) are relevant whenever the ortho/para ratio of H_2 is high. It would be useful to identify the astrophysical cases where rotationally excited ortho-H_2 is relevant for observations of para-H_2O and where more extensive calculations should be carried out to complete the collisional sets provided here.

We are currently carrying out similar calculations for ortho-H_2O with ortho-H_2 ($j_2 = 1, 3$) and for para-H_2O with para-H_2 ($j_2 = 0, 2$).

Acknowledgements. Most scattering calculations were performed at the IDRIS-CNRS and CINES under project 2006-07-08-09 04 1472. This research was supported by the CNRS national program "Physique et Chimie du Milieu Interstellaire" and by the FP6 Research Training Network "Molecular Universe", contract Number: MRTN-CT-2004-512302.

References

Agg, P. J., & Clary, D. C. 1991a, J. Chem. Phys., 95, 1037
Agg, P. J., & Clary, D. C. 1991b, Molecul. Phys., 73, 317
Dabrowski, I. 1984, Can. J. Phys., 62, 1639
Dubernet, M.-L., & Grosjean, A. 2002, A&A, 390, 793
Dubernet, M., Grosjean, A., Daniel, F., et al. 2006, in Ro-vibrational Collisional Excitation Database : BASECOL – http://basecol.obspm.fr, Japan: J. Plasma Fusion Res. Ser., 7
Dubernet, M.-L., Daniel, F., Grosjean, A., et al. 2006, A&A, 460, 323
Dubernet, M.-L., Daniel, F., Grosjean, A., & Lin, C. Y. 2009, A&A, 497, 911
Faure, A., Valiron, P., Wernli, M., et al. 2005, J. Chem. Phys., 122, 221102
Faure, A., Crimier, N., Ceccarelli, C., et al. 2007, A&A, 472, 1029
Flower, D. R. 1999, J. Phys. B Atom. Molecul. Phys., 32, 1755
Flower, D. R. 2001, J. Phys. B Atom. Molecul. Phys., 34, 2731
Flower, D. R., & Launay, J. M. 1985, MNRAS, 214, 271
Flower, D. R., & Roueff, E. 1999a, MNRAS, 309, 833
Flower, D. R., & Roueff, E. 1999b, J. Phys. B Atom. Molecul. Phys., 32, 3399
Green, S., Maluendes, S., & McLean, A. D. 1993, ApJS, 85, 181
Grosjean, A., Dubernet, M.-L., & Ceccarelli, C. 2003, A&A, 408, 1197
Hutson, J. M., & Green, S. 1994, MOLSCAT computer code,version 14, United Kingdom: Collaborative Computational Project No. 6 of the Science and Engineering Research Council
Kłos, J., & Lique, F. 2008, MNRAS, 390, 239
Kyrö, E. 1981, J. Mol. Spectrosc., 88, 167
Mandy, M. E., & Martin, P. G. 1993, ApJS, 86, 199
McBane, G. 2004, MOLSCAT computer code, parallel version (USA: G. McBane)
Mengel, M., de Lucia, F. C., & Herbst, E. 2001, Can. J. Phys., 79, 589
Phillips, T. R., Maluendes, S., McLean, A. D., & Green, S. 1994, J. Chem. Phys., 101, 5824
Phillips, T. R., Maluendes, S., & Green, S. 1996, ApJS, 107, 467
Wernli, M., Valiron, P., Faure, A., et al. 2006, A&A, 446, 367